Minimum Loss Control of a Five-phase Permanent Magnet Assisted Synchronous Reluctance Motor under Open Phase Fault

Akm Arafat Advanced Engineering Cummins Incorporation Fridley, MN, USA aa188@zips.uakron.edu Md. Khurshedul Islam Department of ECE Mississippi State University Starkville, Mississippi, USA mi264@msstate.edu Kazi Nishat Tasnim Department of ECE Mississippi State University Starkville, Mississippi, USA kt1446@msstate.edu Seungdeog Choi Department of ECE Mississippi State University Starkville, Mississippi, USA seungdeog@ece.msstate.edu

Abstract—In this paper, the efficiency of a five-phase Nd- based permanent magnet assisted synchronous reluctance motor has been analyzed to perform optimal efficiency control under different two-phase open fault (TPF) conditions. Since in a PMaSynRM, the torque is generated primarily due to the saliency, under phase lost conditions, the performance of this machine deteriorates heavily. The major reasons behind this are the 1) phase lost condition creates non-uniform flux distribution in the airgap, 2) remaining phase currents become unbalanced, 3) unexpected current harmonics show up, and 4) optimal control angle shifts from its original. With all these effects, the PMaSynRM performs very inefficiently. Therefore, the maximum efficiency control becomes critical. However, maintaining maximum efficiency in the TPF condition is challenging, which requires a smart, fast, and adaptive control strategy to perform a smooth long-term operation. In this paper, particular attention is given to developing an analytical fault model followed by finite element modeling, which is utilized to calculate the efficiency accurately of the PMa-SynRM under faults. Also, an advanced control method has been adopted to continue the maximum efficiency control in those faults.

Keywords: Five-phase PMa-SynRM, current control, vector control, maximum efficiency control.

I.INTRODUCTION

The research interest in multi-phase motors has been growing in recent years as it provides superior performance compared to conventional three-phase motors. With the multi-phase motor, lower torque pulsations can be obtained along with lower current per phase without increasing the voltage per phase [1]. The most important feature of the multiphase motors is the reliability during the fault condition. When a fault occurs in one or more phases in multi-phase motors, it can still operate with remaining healthy phases without any additional hardware [2]. Due to the fault-tolerant capability, multi-phase motors can be a potential candidate for critical areas like automotive, aerospace and naval applications [3].

However, under fault-tolerant operation, the multiphase motors become inefficient. It is very challenging to predict the efficiency and provide a suitable control at critical faults such as open phase faults where the system completely loses one or multiple legs. Therefor providing fault-tolerant control with optimal performance is important. A dynamic current phase advance technique has been developed in previous literature to maximize torque in fault conditions of a five-phase PMa-SynRM [4]. Here, the maximization of the mean

toque is given top priority. Torque ripple minimization of a five-phase PMa-SynRM has been done under open phase faults and considering unbalanced phase resistance [5]. Here, the harmonic suppression is done in the phase current. These methods haven't accounted for the efficiency of the system under faults. In [6], current and torque ripple in a faulted condition of a five-phase PMSM are successfully reduced with a three-level inverter topology utilizing PDPWM control method for generating switching pulses. In [7], the SVM-MPTC scheme has been applied to increase fault-tolerant capability of a five-phase PMSM under open-circuit fault condition, which enabled the system to achieve improved steady-state performance and reduced harmonics. In this article, the cost function is optimized, and the complexity of the algorithm is reduced as the voltage tracking error is minimized. But, there is no indication of maximizing the efficiency in faulty conditions.

There are few researches have been accomplished focusing on efficiency control in permanent magnet machines. In [8], efficiency comparison has been done between three and fivephase PMa-SynRM drive for healthy conditions. In [9], the motor's performance in the faulty condition is improved through voltage feedforward compensator which is based on the relation between the back EMF and faulted phase current. A half-cycle optimal current control (HCOCC) technique has been developed for fault conditions of five-phase IM which reduced copper loss by 50% compared to a conventional current control technique [10]. In [11], electromagnetic, mechanical, and thermal analysis have been done in healthy and open circuit faulted conditions, considering adjacent and non-adjacent phase faults. One major challenge of this method is that the temperature rises too high in an adjacent fault condition. However, there has not been any significant contribution to the efficiency analysis of a five-phase-PMa-SynRM under open phase fault conditions.

In this paper, a comprehensive mathematical analysis of the efficiency under different two-phase fault conditions has been attempted. Based on the analytical outcome, a novel maximum efficiency control under faults has been developed for five-phase PMa-SynRM. The control algorithm is finally integrated with the overall motor control strategy to optimize system efficiency under faults. A detailed MATLAB modeling and Finite Element Analysis (FEA) simulation are carried out to evaluate the proposed strategy's performance. Experimental results are provided to confirm the proposed method.

II. EFFICIENCY CALCULATION UNDER TWO-PHASE OPEN FAULTS

A. Open Phase Fault modeling

Fig.1 shows the different open phase faults, which are considered in the efficiency calculation.

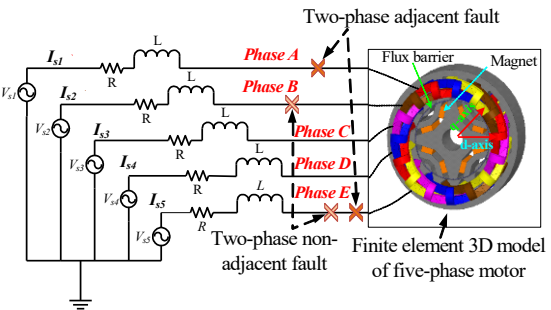


Fig.1. Five-phase system with different open phase faults.

Under two-phase adjacent fault (TPAF) and two-phase nonadjacent fault (TPNF) conditions, there are non-sinusoidal currents in the five-phase PMa-SynRM which represents an unbalanced system. Typically, the total currents can be modeled as,

$$I_T = I_a + I_F \tag{1}$$

 $I_T = I_a + I_F \eqno(1)$ where, I_T , I_a and I_F are the total current, phase current and fault current, respectively. The fault current is generated due to the system unbalance and causes additional losses.

B. Analysis of Efficiency under Fault conditions

In this section, the faulty five-phase PMaSynRM is modeled in the synchronously rotating frame.

First, the balanced electrical drive system is represented in the d- and q- axis coordinate system, which rotates synchronously with the electrical speed, as shown in Fig. 2. Under different faults, the back-emf would have unexpected harmonics as well as there would be non-zero and zero sequence current component (ZSC). Both of them would add unexpected losses in the system. This effect could be modeled as in Fig. 3.

These equivalent circuits represent the effect of copper and iron loss by an armature (Ra) and core resistance (Rc), respectively. An additional back emf content that arises due to the fault has been added in Fig. 3 (edf is the d-axis harmonic and eqf is the q-axis harmonic). These models are utilized to calculate motor efficiency under faults. From Fig. 3, the voltage equations can be developed as follows:

$$v_{d} = R_{a}i_{od} - (1 + R_{a}/R_{c})\omega L_{q}i_{oq} + (1 + R_{a}/R_{c})\omega\psi + e_{df}$$

$$v_{q} = R_{a}i_{oq} + (1 + R_{a}/R_{c})\omega L_{d}i_{od} + e_{qf}$$

$$v_{o} = i_{o}R_{o}$$
(2)

The current equations can be derived as follows

$$i_{cd} = -\omega L_q i_{oq} + \omega \psi / R_c$$

$$i_{cq} = \omega L_d i_{od} / R_c$$

$$i_{co} = i_{o}R_{ao}/R_{c} + R_{ao}$$

$$i_{od} = i_d - i_{cd}$$

$$i_{oq} = i_q - i_{cq}$$

$$i_o = i_{oo} + i_{co} \tag{3}$$

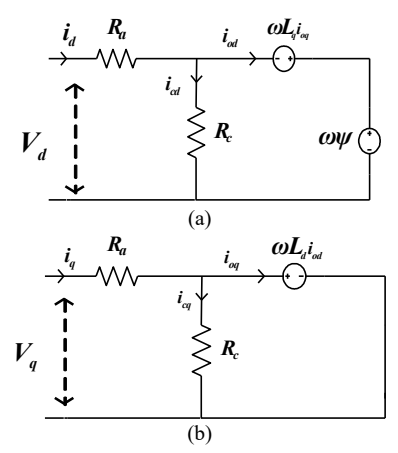


Fig. 2. d- and q- axis equivalent circuit of five-phase PMa-SynRM in healthy condition. (a) d-axis (b) q-axis.

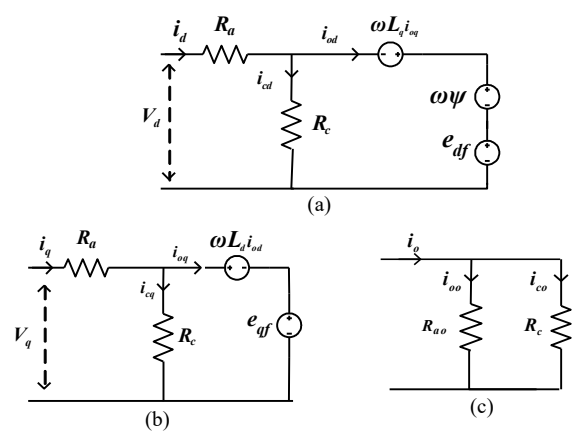


Fig. 3. d, q, and 0-axis equivalent circuits of five-phase PMa-SynRM at faulty condition, (a) d-axis (b) q-axis (c) 0-axis

where, i_d , i_q , and i_o are d, q, and zero axis components of armature current, i_{cd} , i_{cq} , and i_{co} are d, q, and zero axis components of iron loss current, v_d , v_q , and v_o are d, q, and zero axis components of the terminal voltage. L_d and L_q are the d- and q- axis component of the armature. R_a and R_c are the armature winding resistance per phase and core loss resistance. The output electromagnetic torque can be derived

$$T = 5P/2\left\{\psi i_{od} + \left(L_d - L_q\right) i_{oq} i_{od}\right\} + \Delta\tau \tag{4}$$

where $\Delta \tau$ is the contribution due to the harmonics, P, w, and Ψ are the number of rotor poles, electrical speed, and permanent magnet flux linkage, respectively. The electrical loss of five-phase PMa-SynRM (iron loss and copper loss) and Mechanical can be expressed as:

$$W_E = W_{cu} + W_{fe} \tag{5}$$

$$W_{cu} = R_a \left(i_d^2 + i_q^2 + i_o^2 \right) \text{ and } W_{fe} = R_c \left(i_{cd}^2 + i_{cq}^2 + i_{co}^2 \right)$$
 $W_m = T_{mech} w_r$ (6)

where T_{mech} and w_r are friction torque and mechanical angular speed $w_r = w/2p$. The total loss, output power, and efficiency are derived as,

$$W_T = W_{cu} + W_{fe} + W_m$$

$$P_{out} = Tw_r$$

$$\eta = 100 P_{out} / (P_{out} + W_T)\%$$
(7)

Using (7), the healthy condition efficiency can be calculated as follows,

$$h = 100Tw/P R_o \underbrace{\frac{3}{2} \frac{wy}{R_c} - L_q i_{oq} w}_{R_c} \underbrace{\frac{3}{2} + \frac{3}{2} \frac{2L_d Tw}{5R_c P(y_m + i_{oq} x) \frac{3}{2} \frac{3}{2} \frac{3}{2}}_{\frac{3}{2} + \frac{3}{2} \frac{3}{2} \frac{3}{2} \frac{3}{2}} + \frac{3}{2} \underbrace{\frac{3}{2} \frac{3}{2} \frac{3}{2}}_{\frac{3}{2} + \frac{3}{2} \frac{3}{2} \frac{3}{2} \frac{3}{2} \frac{3}{2}}_{\frac{3}{2} + \frac{3}{2} \frac{$$

Here, $x = L_d - L_q$ and i_{od} is expressed as a function of i_{oq} from equation (4) that allows the efficiency to be a function of only i_{oq} .

Similarly, the efficiency at faulty condition can be derived as follows,

$$\eta = 10.5T\omega / \begin{cases} 5R_{a} \left(\frac{e_{df} + \omega \psi_{m} - L_{q}i_{oq}\omega}{R_{c}} + \frac{2T}{5P(\psi_{m} + i_{oq}x)} \right)^{2} + \left(\frac{e_{qf} + \frac{2L_{d}T\omega}{5P(\psi_{m} + i_{oq}x)}}{R_{c}} \right)^{2} + i_{o}^{2} \right) \\ R_{c} \left(\frac{e_{df} + \omega \psi_{m} - L_{q}i_{oq}\omega}{R_{c}} \right)^{2} + \left(\frac{e_{ef} + \frac{2L_{d}T\omega}{5P(\psi_{m} + i_{oq}x)}}{R_{c}} \right)^{2} + \left(\frac{R_{g}i_{o}}{R_{a} + R_{c}} \right)^{2} \right) + \omega \left(\frac{T_{mech}}{P} + \frac{20T}{191} \right) \end{cases}$$

The analytical efficiency plot is shown in Fig. 4. Fig. 4 (a) shows the efficiencies under healthy, and TPAF faulty conditions follow parabolic paths. At rated i_{oq} , the efficiency under healthy condition is higher than the efficiency at faulty condition. It is found that to achieve maximum efficiency under TPAF faulty condition, a higher i_{oq} compared to rated

 i_{oq} is needed. Fig. 4 (b) shows the efficiency versus the speed. It is observed that the efficiency under the healthy condition at any speed is higher than the efficiency under the TPAF fault condition. Fig. 4 (c) shows the efficiencies at different load conditions and the fault currents. The efficiency reduces as the fault current increases at any loads.

C. Minimal Currents for maximum Efficiency under faults

In an electrical machine, the mechanical loss is depended on the application and environment, which is not controllable. On the other hand, the electrical loss is controllable and can be minimized by applying an optimal current vector. This optimal current vector ensures the maximum efficiency of the machine. During the fault condition, W_E can be expressed as a function of i_{od} , i_{oq} , i_{oo} , and w by using (5). The condition of minimal currents for maximum efficiency under fault condition can be derived from (8) as follows

$$d\eta/di_{oq} = 0 \tag{10}$$

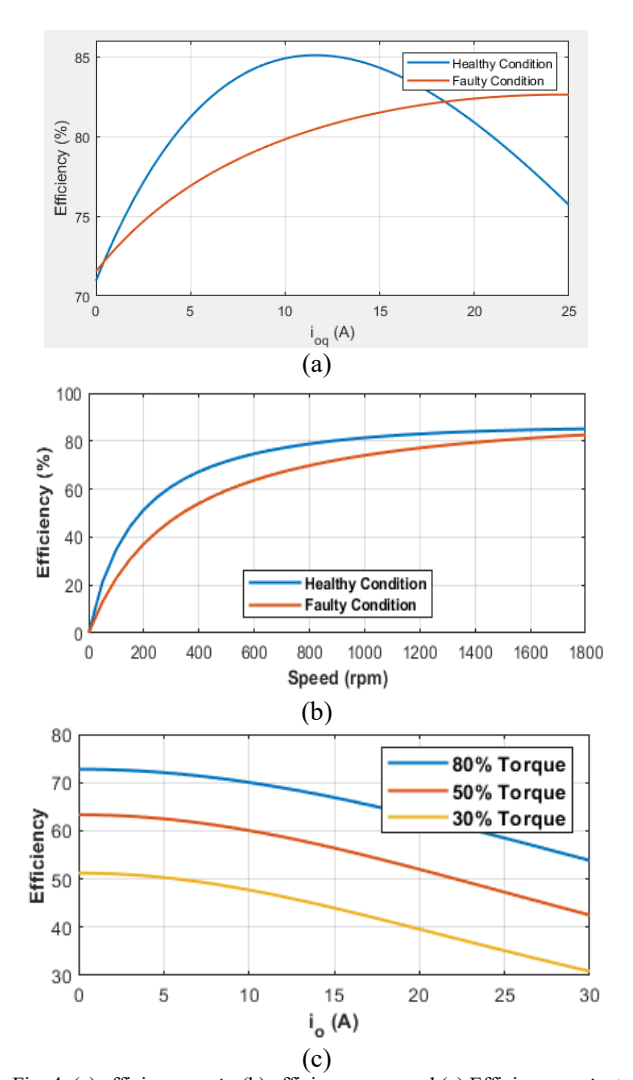


Fig. 4. (a) efficiency vs i_{oq} (b) efficiency vs speed (c) Efficiency vs i_o at healthy and faulty condition.

If we consider $L_d=L_q$ i.e., no saliency in the machine, then a solution of (10) gives the first-order equation of i_{oq} . But, the studied machine has saliency as $L_d>L_q$, which results in a fourth-order quadratic equation of i_{oq} as follows,

$$Ai_{oq}^{4} + Bi_{oq}^{3} + Ci_{oq}^{2} + Di_{oq} + E = 0$$
Where,
$$A = -50P^{2}L_{d}L_{a}x^{3}\omega^{2} - 50P^{2}R_{c}L_{a}^{2}\omega^{2}x^{3}$$
(11)

$$\begin{split} B &= -50P^2L_q^2\omega^2x^2\psi_m - 100P^2x^2\omega^2\psi_mL_qL_d - 150P^2R_cL_q^2\omega^2\psi_mx^2 \\ C &= -100P^2L_q^2\omega^2\psi_mx - 50P^2L_qL_dx\omega^2\psi_m^2 - 150P^2R_cL_q^2\omega^2x\psi_m^2 \\ D &= 100R_aL_dT\omega xR_cPx - 500R_aR_ce_{qf}P^2x\psi_m^2 - 200R_aR_cP\psi_mxL_dT\omega \\ &+ 150P^2\psi_m^2L_q\omega e_{df}x - 100P^2L_q^2\omega^2\psi_mTxR_c + 40PL_q\omega\psi_mxTR_c \\ &+ 150P^2R_cL_q\omega e_{df}x\psi_m^2 \\ E &= 100R_aL_dT\omega R_cP + 100R_aL_dT\omega xPe_{qf}\psi_m + 40R_aL_d^2T^2\omega^2x \\ &- 100R_aR_cP\psi_m^2L_dT\omega + 100P^2\psi_me_{df}L_q\omega TxR_c + 100P^2\psi_m^2\omega^2L_qTxR_c \\ &+ 20PL_a\omega\psi_m^2TR_c + 40PL_a\omega T^2xR_c^2 + 20L_dT\omega xe_{qf}P\psi_m + 8L_d^2T^2\omega^2x \end{split}$$

After solving (11), the real positive i_{oq} has been considered to find maximum efficiency under faults.

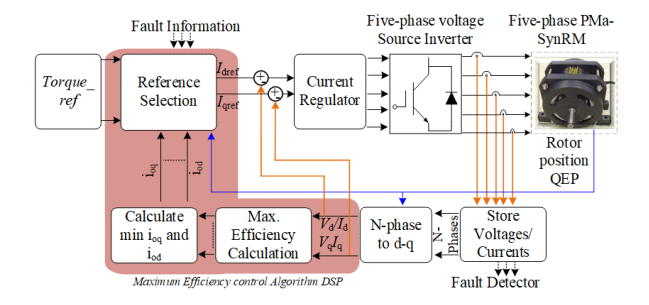


Fig. 5. The control strategy of the five-phase five-phase PMa-SynRM integrated with the loss minimization technique.

III. CONTROL STRATEGY FOR MAXIMUM EFFICIENCY UNDER FAULTS

The efficiency calculation method described in the previous section is used to control five-phase PMa-SynRM. Fig. 5 shows the block diagram of the overall control strategy using the loss minimization algorithm. The d and q-axes reference currents (I_{dref} and I_{qref}) have been generated based on the reference torque and control optimal current i_{oq} . The adaptive control signal i_{oq} is generated based on the optimal efficiency point which is found from (11).

Based on the reference d-q axis current, the current controller generates the d and q-axes reference voltages (V_{dref} and V_{qref}). The phase currents, voltages, and position (θ) have been taken as feedback. Depending on the current magnitude, the fault type of the five-phase PMa-SynRM has been determined in the fault detection block. These motor currents and voltages are converted to d-q voltages and currents. The currents are used in the current controller block to find the error signal. The measured speed is used as feedback in the speed controller loop.

IV. SIMULATION RESULTS

Table I.	SPECIFICATIONS

Value
15.2A
67.0V
15.17Nm
1800 rpm
0.30 ohm
3.00 kW

The proposed model has been simulated in Matlab/Simulink and Ansys Maxwell Finite element analysis (FEA). The TPAF and TPNF conditions have been run at 1800 rpm with full loads and 300 rpm with 30% load.

Fig. 6(a)-(d) show the healthy condition motor phase currents, magnetic saturation and torque speed curve obtained through FEA and Matlab.

Fig. 7 (a)-(d), shows the phase currents analysis at TPAF condition. Fig. 7 (a) shows the phase current under TPAF. Fig. 7 (b) show the phase currents with optimal i_{oq} . Fig. 7 (c) show the phase currents harmonics under TPAF. Fig. 7 (d) show the phase currents of the machine with optimal i_{oq} . It is observed certain harmonics (3rd and 5th) are suppressed with the proposed method, therefore increasing the efficiency.

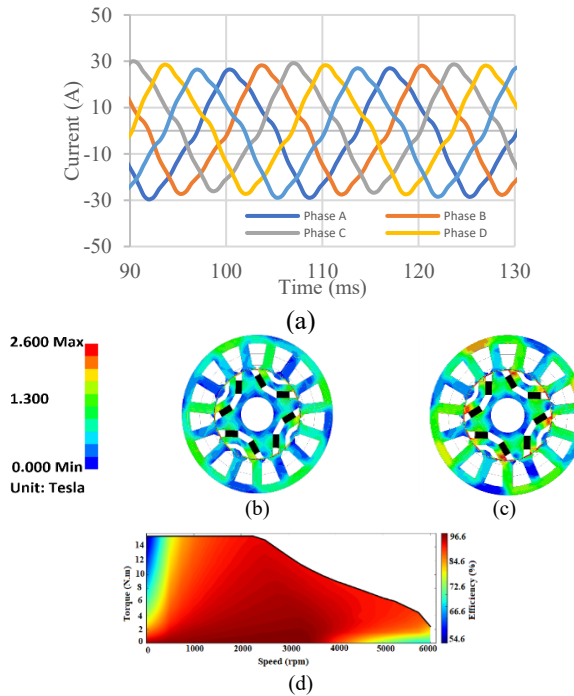
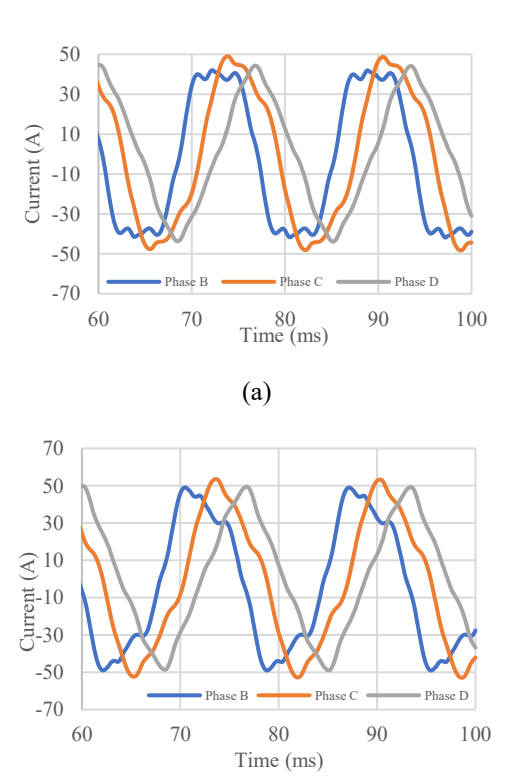


Fig. 6. Waveform of the phases under healthy condition (a) phase currents, (b) magnetic flux density at a healthy condition (c) magnetic flux density TPAF (h) efficiency map.

Fig. 8 (a)-(d), shows the phase currents analysis at the TPNF condition. Fig. 7 (a) shows the phase current under TPNF. Fig. 8 (b) show the phase currents with optimal i_{oq} . Fig. 8 (c) shows the phase currents harmonics under TPNF. Fig. 8 (d) show the phase currents of the machine with optimal i_{oq} . It is observed certain harmonics (3rd and 5th) are suppressed with the proposed method, therefore increasing the efficiency.



(b)

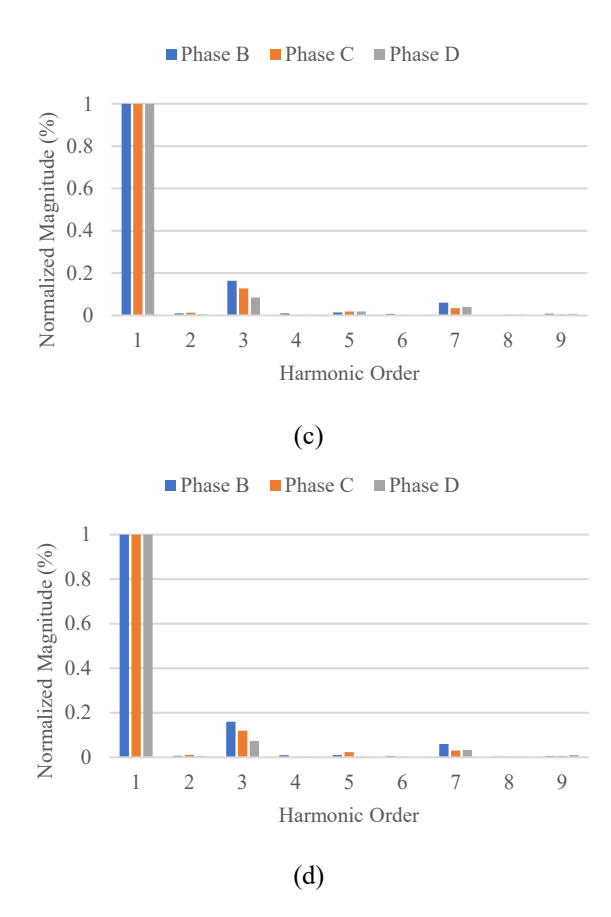
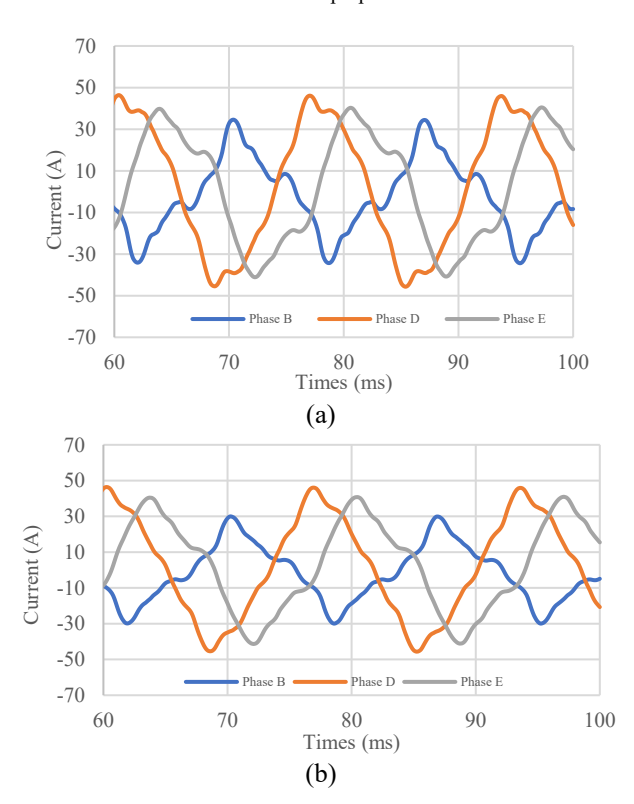
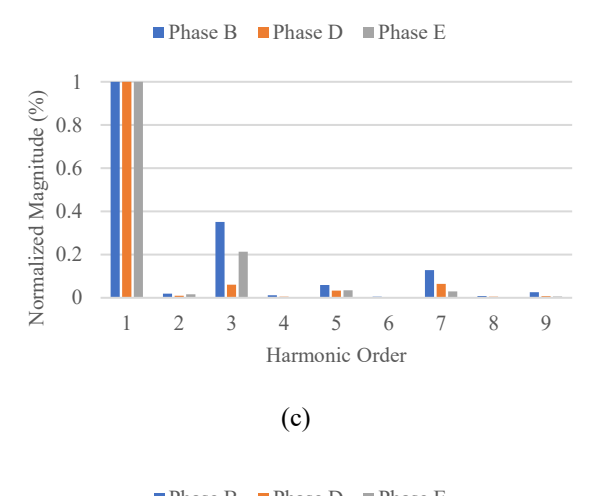


Fig. 7. Current waveform at two phase adjacent (rated condition), (a) at fault, (b) with proposed method, (c) harmonic orders at faults, and (d) harmonic orders with proposed method.





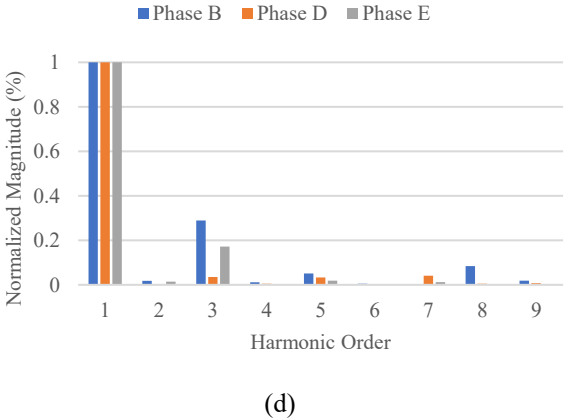


Fig. 8. Current waveform at two-phase non-adjacent (rated condition), (a) at fault, (b) with proposed algorithm, (c) harmonic orders at faults, and (d) harmonic orders with the proposed method.

TABLE II. THD COMPARISON			
Conditions	At Fault	With the proposed	
		method	
TPAF at rated	Phase B= 17.64%	Phase $B = 17.10\%$	
	Phase $C = 13.45\%$	Phase $C = 12.21\%$	
	Phase D = 9.6%	Phase D = 8.01%	
TPNF at rated	Phase B = 36.22%	Phase $B = 35.10\%$	
	Phase $D = 10.20\%$	Phase $D = 9.40\%\%$	
	Phase $E = 22.1\%$	Phase $E = 20.4\%$	
TPAF at 30%	Phase B = 14.1%	Phase $B = 12.55\%$	
rated	Phase $C = 9.8\%$	Phase $C = 8.3\%$	
	Phase D = 7.9%	Phase D = 7.9%	
TPNF at 30%	Phase B = 24.76%	Phase B = 13.95%	
rated	Phase D = 13.5%	Phase D = 12.1%	
	Phase E = 25.3%	Phase E = 14.4%	

The total harmonic distortion at various faults is summarized in Table II. At rated condition, the THD under TPAF has improved at an average of 1.13% with the proposed method. Under TPNF, the average improvement is found as 1.21%. At 30% rated condition, the THD under TPAF has improved at an average of 1.21% with the proposed method. Under TPNF, the average improvement is found as 7.7%.

The efficiency is calculated at various fault conditions and given in Table III.

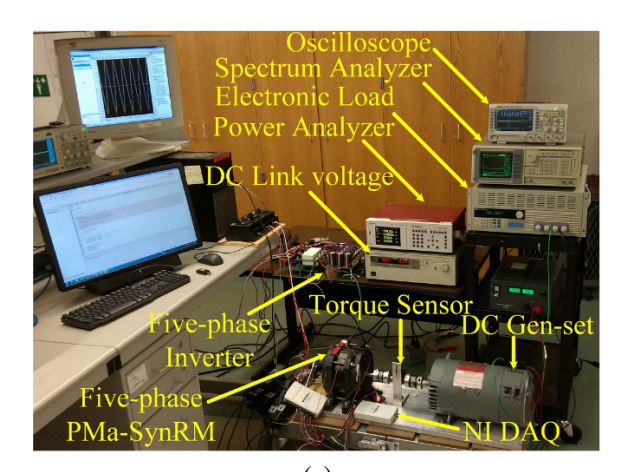
T III	DEPLOID LON	COMPARISON
IARIFIII	EFFICIENCY	COMPARISON

Conditions	At fault	With proposed method
TPNF at 1800 rpm	68.8%	71.5%
TPNF at 1800 rpm	71.2%	74.3%
TPAF at 300 rpm	70.7%	71.2%
TPNF at 300 rpm	76.5%	80.45%

The efficiency clearly showed a clear positive indication of using the proposed method with an improvement of $\sim 3\%$ in both TPAF and TPNF condition under rated operation. The efficiency improved $\sim 4\%$ in TPNF condition at 30% rated operation.

V. EXPERIMENTAL RESULTS

The proposed method is verified in a dyno test bed that includes a five-phase PMa-SynRM, a five-phase voltage source inverter and a DC motor as load. The five-phase motor controller has a TI DSP F28335, five current sensors, and an encoder for the position measurement. Fig. 9 shows the experimental environment that has been utilized in this experiment.



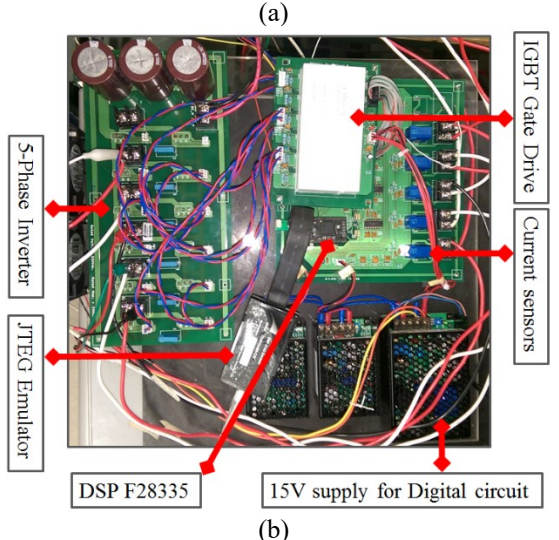


Fig. 9. Experimental results: (a) test setup, (b) inverter with controller.

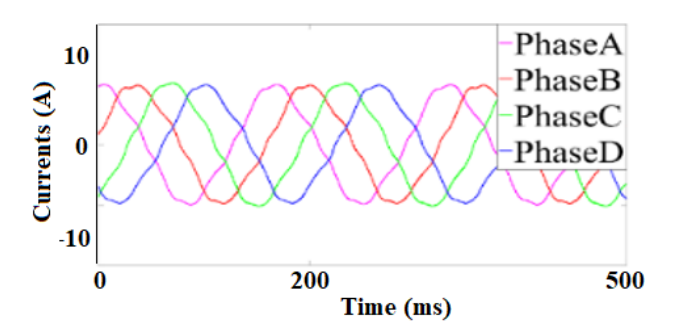
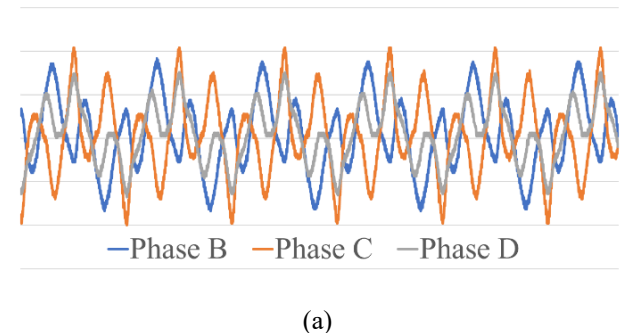
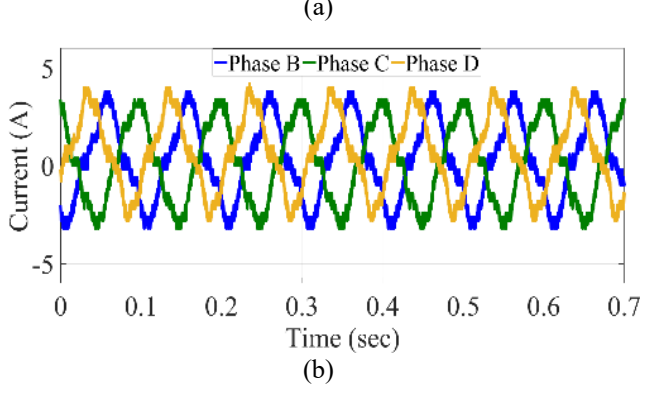
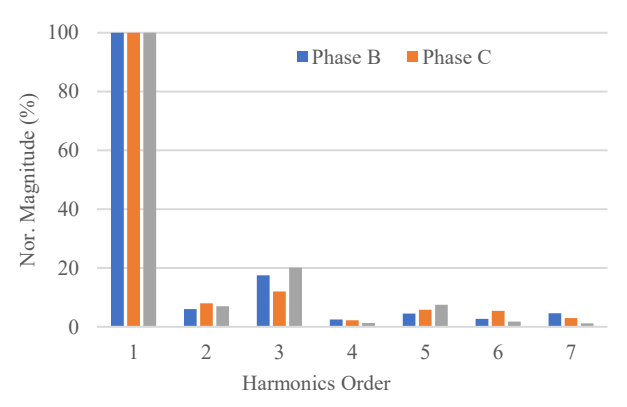


Fig. 10. Healthy phase currents.

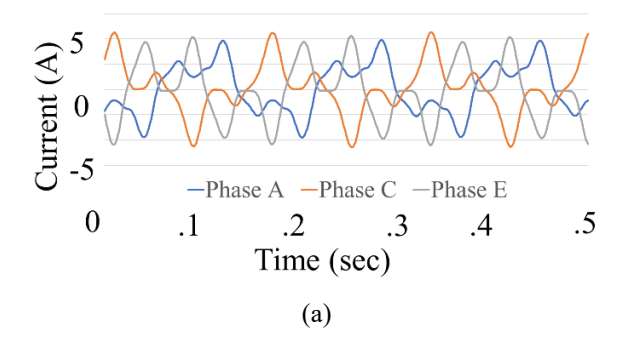
Fig. 11 shows the phase currents when operating at two-phase adjacent faults. Fig. 11 (a) shows the phase current under the TPAF condition. Fig. 11(b) shows the phases currents with the proposed method. Fig. 11(c) shows the FFT of Fig. 11(b).

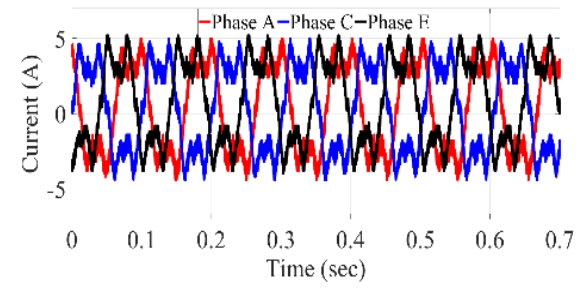






(c)
Fig. 11. Current waveform at two phase adjacent (30% rated condition),
(a) at fault, (b) with proposed algorithm, and (d) harmonic orders with proposed method.





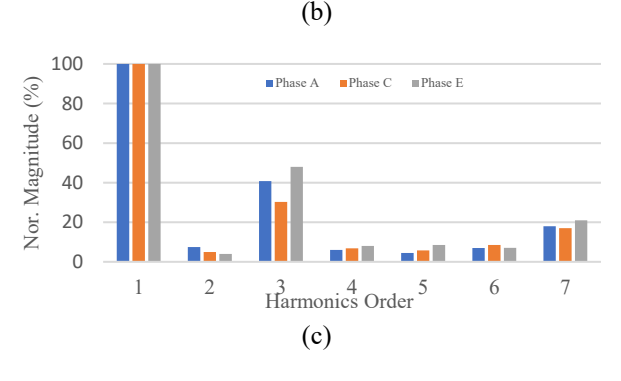


Fig. 12. Current waveform at two phase non adjacent (30% rated condition), (a) at fault, (b) with proposed algorithm, and (d) harmonic orders with proposed method.

Fig. 12 shows the phase currents when operating at two phase non-adjacent faults. Fig. 12 (a) shows the phase current under TPNF condition. Fig. 12(b) shows the phases currents with the proposed method. Fig. 12(c) shows the FFT of Fig. 12(b).

TABLE IV: SUMMARY CACULATION

	TPAF		TPNF			
Parameters	Phase B	Phase C	Phase D	Phase A	Phase C	Phase E
THD (%)	22.74	15.16	29.66	38.99	38.77	45.79
RMS Current (A)	2.084	2.066	1.915	2.863	2.791	2.690

TABLE V. EFFICIENCY COMPARISON

TABLE V. EFFICIENCY COMPARISON			
Conditions	At fault	With proposed	
		method	
TPAF at 300 rpm	64.2%	84.3%	
TPNF at 300 rpm	70.1%	83.8%	

Table IV and V show the summary of the current calculation and efficiency comparison. With the proposed method, the efficiency under TPAF and TPNF improved by 20.1% and 13.7%, respectively.

VI. CONCLUSION

In this study, the efficiency of a five-phase PMa-SynRM under two-phase open faults have been analyzed through theory, simulation, and experimental results. From simulations, it has been found that using the proposed method, the efficiency of the five-phase PMa-SynRM under various faults is improved by ~3-4% when operating at rated condition. The experimental test carried at 30% rated condition. In this condition, the efficiency improved by 20.1% and 13.7% with the proposed method. It is found that the proposed method can significantly improve the efficiency of the five-phase drive under critical faults.

VII. REFERENCES

- [1] S. Dwari and L. Parsa, "An Optimal Control Technique for Multiphase PM Machines Under Open-Circuit Faults," in IEEE Transactions on Industrial Electronics, vol. 55, no. 5, pp. 1988-1995, May 2008.
- [2] A. Mohammadpour, S. Mishra and L. Parsa, "Fault-Tolerant Operation of Multiphase Permanent-Magnet Machines Using Iterative Learning Control," in IEEE Journal of Emerging and Selected Topics in Power Electronics, vol. 2, no. 2, pp. 201-211, June 2014.
- [3] L. Parsa and H. A. Toliyat, "Sensorless Direct Torque Control of Five-Phase Interior Permanent-Magnet Motor Drives," in IEEE Transactions on Industry Applications, vol. 43, no. 4, pp. 952-959, July-aug. 2007.
- [4] A. K. M. Arafat and S. Choi, "Optimal Phase Advance Under Fault-Tolerant Control of a Five-Phase Permanent Magnet Assisted Synchronous Reluctance Motor," in IEEE Transactions on Industrial Electronics, vol. 65, no. 4, pp. 2915-2924, April 2018.
- [5] A. K. M. Arafat and S. Choi, "Torque ripple minimization of a five-phase permanent magnet assisted synchronous reluctance motor under open phase faults," 2017 IEEE Applied Power Electronics Conference and Exposition (APEC), Tampa, FL, 2017, pp. 1928-1934.
- [6] A. A. Gandomi, S. Saeidabadi and L. Parsa, "A Fault Tolerant T-type Inverter for Five-phase PMSM Drives," IECON 2019 45th Annual Conference of the IEEE Industrial Electronics Society, Lisbon, Portugal, 2019, pp. 834-839
- [7] Huang, W. Hua, F. Chen, M. Hu and J. Zhu, "Model Predictive Torque Control With SVM for Five-Phase PMSM Under Open-Circuit Fault Condition," in IEEE Transactions on Power Electronics, vol. 35, no. 5, pp. 5531-5540.
- [8] A. Arafat and S. Choi, "Comparison of electrical losses in an inverter-fed five-phase and three-phase permanent magnet assisted synchronous reluctance motor," 2016 IEEE Applied Power Electronics Conference and Exposition (APEC), Long Beach, CA, 2016, pp. 2847-2854.
- [9] H. Zhou, G. Liu, W. Zhao, X. Yu, and M. Gao, "Dynamic Performance Improvement of Five-Phase Permanent-Magnet Motor With Short-Circuit Fault," in IEEE Transactions on Industrial Electronics, vol. 65, no. 1, pp. 145-155, Jan. 2018.
- [10] E. Mahmoud, A. Abdel-Khalik and H. Soliman, "An improved fault tolerant for a five-phase induction machine under open gate transistor faults", Alexandria Engineering Journal, vol. 55, no. 3, pp.
- [11] P. T. Luu, J. Lee, Y. Jeong, J. Kim, J. Lee and K. Lee, "Investigation of Multi-Physical Characteristics in Coupling-Five-Phase Motor under Driver-Open-Phase Fault Condition for Small Propulsion System," 2019 22nd International Conference on Electrical Machines and Systems (ICEMS), Harbin, China, 2019, pp. 1-4.